EARTH SURFACE PROCESSES AND LANDFORMS
Earth Surf. Process. Landforms **45**, 1705–1716 (2020)

Published online 11 March 2020 in Wiley Online Library
(wileyonlinelibrary.com) DOI: 10.1002/esp.4840

Dust provenance and its role as a potential fertilizing agent for the Okavango Delta, Botswana

Marc S. Humphries,[1*] Claudia R. Benitez-Nelson,[2] Michael Bizimis,[2] Timothy J. Ralph,[3] Zacchary T. Larkin[3] and Terence S. McCarthy[4]
[1] School of Chemistry, University of the Witwatersrand, Johannesburg, South Africa
[2] School of the Earth, Ocean and Environment, University of South Carolina, Columbia, SC USA
[3] Department of Environmental Sciences, Macquarie University, Sydney, NSW Australia
[4] School of Geosciences, University of the Witwatersrand, Johannesburg, South Africa

Received 31 July 2019; Revised 23 January 2020; Accepted 4 February 2020

*Correspondence to: Marc S. Humphries, School of Chemistry, University of the Witwatersrand, Johannesburg, South Africa. E-mail: marchump@gmail.com

ESPL
Earth Surface Processes and Landforms

ABSTRACT: Dust plays a globally important role in supplying biologically essential elements to landscapes underlain by nutrient-poor substrates. Here we show that dust may play a significant role in sustaining productivity in the vast wetlands of the Okavango Delta in southern Africa, one of the world's richest biodiversity hotspots. Dust accumulates preferentially on tree-covered islands in the seasonal swamps of the Delta, creating pockets of fine-grained, nutrient-rich material within the semi-arid landscape of the Kalahari Desert. Strontium and neodymium isotopes reveal that this dust likely originates predominantly from the Makgadikgadi salt pans, located 300 km away, and contributes 10–80% of the fine-grained material present in Okavango island soils. Surface material sourced from the Makgadikgadi Pans contains relatively high amounts of bioavailable phosphorus and iron, potentially influencing Okavango Delta biological productivity. We propose that long-term ecosystem productivity and nutrient availability in the Okavango may be strongly mediated by regional dust inputs. Understanding the influence of dust deposition on nutrient loads and biogeochemical cycling is thus critical for predicting the response of the Okavango Delta to future changes in climate. We suggest that dust inputs may play a significant role in the supply of nutrients to other large, global wetland systems located in dryland environments. © 2020 John Wiley & Sons, Ltd

KEYWORDS: dust transport; Kalahari Desert; Makgadikgadi; nutrient enrichment; Okavango Delta; radiogenic isotopes; wetlands in drylands

Introduction

The Okavango Delta in northern Botswana (Figure 1) is one of the world's richest biodiversity hotspots (Junk et al., 2006; Ramberg et al., 2006). The annual flood wave that traverses the 25 000 km^2 alluvial fan inundates extensive areas of permanent and seasonally flooded swamp, sustaining one of the most pristine wetland ecosystems on earth (Allan et al., 2017). These vast swamplands stand in stark contrast to the surrounding semi-arid and nutrient-poor landscape. The Delta lies on the edge of the Kalahari Desert and is underlain by unconsolidated aeolian sand that blankets much of the region (Thomas and Shaw, 1991). The sandy nature of the catchment and the generally low level of chemical weathering results in a system that is dominated by fine to medium-grained quartz sand and hyperoliotrophic water (Garstang et al., 1998; McCarthy, 2013).

How the Okavango ecosystem supports abundant and diverse vegetation on a sandy, nutrient-poor substrate remains an enigma. It has been hypothesized that aeolian dust may act as a source of nutrients and trace elements that are critical to the functioning of the Okavango ecosystem (Garstang et al., 1998; Krah et al., 2004; Humphries et al., 2014). The often long-range transport of dust is known to play a significant role in the supply of nutrients and biologically essential trace elements to marine and terrestrial ecosystems around the world, including the North Atlantic Ocean (Jickells, 1999; Pabortsava et al., 2017), the Amazon rainforest (Swap et al., 1992; Bristow et al., 2010), Caribbean coral reefs (Muhs et al., 2007), and montane ecosystems (Soderberg and Compton, 2007; Aciego et al., 2017).

In southern Africa, dry or seasonally inundated lake basins in the Kalahari, notably the Makgadikgadi Pans in Botswana and the Etosha Pan in northern Namibia, are recognized as the major sources of dust in the region (Prospero et al., 2002; Washington et al., 2003; Bryant et al., 2007). These two ephemeral lake basins are amongst the southern hemisphere's largest dust sources. Dust production in southern Africa is observed year-round and is carried primarily in a north-westerly direction towards the Atlantic Ocean (Garstang et al., 1998; Prospero et al., 2002). Air-mass trajectory analyses suggest that approximately 11.5 million tonnes of airborne material is transported annually across the Okavango region in anticyclonic circulation systems (Tyson *et al.*, 1996), with aerosol fallout over the Delta estimated at 250 000 tonnes per annum (Garstang et al., 1998). While estimated fallout over the Delta is not supported by measured rates of deposition, calculated fluxes consider only atmospheric contributions under

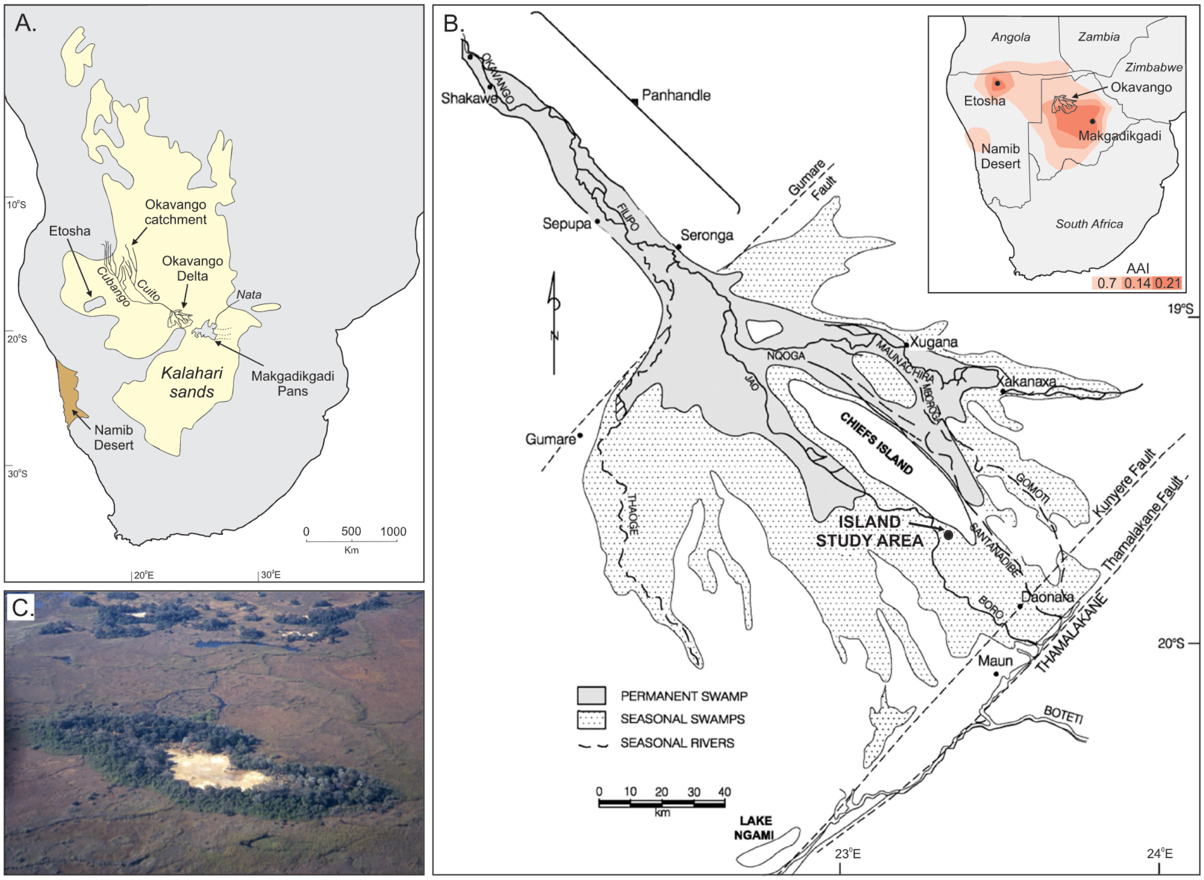

Figure 1. Study area. (A) Map showing the extent of the Kalahari sands (after Thomas and Shaw, 1990) and location of the Okavango Delta in relation to major active dust source areas in southern Africa. (B) The Okavango Delta and location of the islands sampled in the seasonal swamps. Inset shows dust activity over southern Africa derived from total ozone mapping spectrometer (TOMS) data (after Prospero et al., 2002). Orange shading indicates dust concentrations based on the absorbing aerosol index (AAI). Days per month when the AAI equals or exceeds 0.7 are plotted. Note that while TOMS spectral data are often used to study atmospheric dust, they are sensitive to aerosol layer height and cannot fully detect aerosols within 1–2 km above the Earth's surface. (C) A typical island on the Okavango fan, showing the distinct vegetation zonation that characterizes these topographic features. [Colour figure can be viewed at wileyonlinelibrary.com]

anticyclonic flow conditions and thus likely underestimate the total input of airborne material. This dust is suspected to accumulate preferentially on tree-covered islands, which capture wind-blown material (Humphries et al., 2014). Such islands characterize the seasonal swamps of the Okavango, providing potentially important sites for dust-associated nutrient inputs.

Despite being recognized as an important source of dust, the biological fertilization potential of airborne material in southern Africa has largely been overlooked. Understanding the importance of dust is particularly crucial for predicting how large, nutrient-limited ecosystems, such as the Okavango Delta, will respond to climate change and land-use intensification. Here, we use trace element and Sr–Nd isotope compositions to pinpoint the provenance of dust in the Okavango Delta. We show that windblown dust is a significant contributor to soils in the Okavango and argue that dust deposition is a significant source of new nutrients to the ecosystem.

Regional Setting

The Okavango Delta

The Okavango Delta lies within the Kalahari Basin (Figure 1), a large, intracontinental depression spanning some 2.5 million square kilometres that formed during the breakup of Gondwana about 140 million years ago. It has since largely filled with aeolian sand (Thomas and Shaw, 1991; McCarthy, 2013). The uppermost unconsolidated sands, which locally exceed 300 m in thickness, cover large portions of southern Africa and are believed to form the largest continuous sand body on earth (Thomas and Shaw, 1990). The Kalahari Basin and geological development of the Okavango have been profoundly influenced by continued rifting of the African continent. The Okavango Delta lies within a fault-bound depression that has been partly filled by wind-blown sand and sediment brought down by the Okavango River (McCarthy, 2013). In the upper reaches of the Delta, the Okavango River is confined in a narrow (<12 km) depression known as the Panhandle, but divides into several distributary channels farther downstream forming a large, gently sloping alluvial fan. The fan is surrounded by aeolian sand, now largely covered by grassland and savanna, although traces of the former dune fields are evident in areas, particularly along the western and southern edge of the fan.

The Okavango River derives its water from two major tributaries, the Cubango and the Cuito, which flow from the highlands of central Angola. Rainfall in the catchment averages approximately 1000 mm per annum and peaks in the late summer (January to March; Wilson and Dincer, 1976). Rainfall enters the Okavango River via groundwater seepage, resulting in a delayed and extended seasonal flood pulse that is characterized by a steady rise and fall in discharge (McCarthy, 2006). Base flow in the Okavango River is sufficient to sustain about 6000 km^2 of permanent swamp in the upper reach of the fan, but the area of inundation can expand to over 12 000 km^2 with the arrival of the seasonal flood. Short-lived flood events do not occur and seasonal water-level fluctuations in the permanent swamps are small (McCarthy, 2006). The advance of the flood wave across the seasonal floodplains is very slow, occurring mainly by unchannelized sheet flow, and taking 4–5 months to traverse the 250 km length of the fan (McCarthy, 2013). During periods of inundation, water depth in the seasonal wetlands is typically around 30 cm. The fan terminates against faults in the south and only about 1–2% of the total annual inflow leaves the fan as outflow via the Boteti River (McCarthy et al., 1998). The bulk of the water that enters the Delta each year is lost to the atmosphere by evapotranspiration.

The Okavango River catchment is largely underlain by Kalahari sand, although the headwaters of the Cubango tributary drain basement granites (McCarthy, 2013). The sandy nature of the drainage basin results in the Okavango River carrying very low suspended sediment (<12 mg l^{-1}) and solute (~40 mg l^{-1}) loads (McCarthy et al., 1998). The solute load is dominated by silica, calcium and magnesium bicarbonates and nutrients occur at extremely low concentrations, with total nitrogen typically <1 mg l^{-1} (<70 μM) and total phosphorus ~0.05 mg l^{-1} (~1.6 μM; Krah et al., 2006). Despite being characterized by low iron and nutrient concentrations, discharge within the Okavango River (ranging between 6000 and 16 400 Mm^3 year^{-1}; McCarthy, 2013) represents an important contribution to the Delta's nutrient budget. Maximum estimates of the total annual input of total nitrogen and phosphorus by river water is calculated to be around 10 200 and 600 tonnes, respectively (Garstang et al., 1998). However, leakage of water through the peat-lined margins of the upper channels results in water entering the backswamp and distal areas of the swamp being deficient in nutrients (Garstang et al., 1998), with the seasonal floodplains generally considered to be predominantly phosphorus-limited (Ramberg et al., 2010).

Alluvial sediment is derived almost entirely from the erosion of reworked aeolian deposits and consists primarily of quartz-rich, fine to medium sand. Clastic sediment is transported primarily as bedload, with the bulk (~95%) of this material being deposited in the anastomosed reach of the Panhandle (McCarthy et al., 1991). Channel beds consist of fine to medium-grained sand (McCarthy et al., 1991), with margins densely vegetated by grasses, reeds and sedges. Suspended load concentrations in the upper channels are low and consist mainly of kaolinite and quartz, which is filtered out and incorporated into the peat that forms the channel banks. Relatively little clastic sediment is introduced onto the distal seasonally flooded areas of the fan (McCarthy et al., 1991), thus the floodplain soils are predominantly quartz (>97%) and typical of the aeolian sand that surrounds the Delta (McCarthy and Ellery, 1995). The phosphorus and iron content of floodplain soils is low, rarely exceeding 0.04 and 0.4 wt%, respectively (McCarthy et al., 1998).

The topography of the fan surface is gently undulating, with a local relief on the order of 1.5 to 2 m, creating numerous islands that rise above the water by typically less than 1 m. While relatively few islands occur in the permanent swamps, they form an important component of the seasonal swamp where they vary in size from less than 1 m^2 to several thousand square metres (Gumbricht et al., 2004). The origin of the undulating topography that gives rise to islands on the Okavango fan has been studied in detail and the majority of islands appear to either represent abandoned channels or originate through termite activity (Ellery et al., 1993; McCarthy et al., 1998, 2012). Islands remain elevated above the surrounding swamp water level and support vegetation intolerant of flooding (Figure 1C). Once established, islands are thought to grow, in part, through the subsurface accumulation of silica and calcite, which precipitates in response to transpirational water loss (McCarthy et al., 2012). Trees, which are almost exclusively confined to islands, play a particularly important role in lowering the local water table, producing a net inflow of groundwater from the surrounding wetlands. An increase in solute concentration beneath islands produces marked variations in vegetation composition that reflect tolerance to salinity (Ellery et al., 1993). Evergreen tree species are typically found on the outer fringes of islands, while grasses interspersed with sodium carbonate-encrusted bare soil dominate the island interiors.

Regional dust sources

The Southern Hemisphere receives much lower dust inputs compared to the Northern Hemisphere (Prospero et al., 2002). In southern Africa, dust production is observed year-round, with increased activity during late winter (Garstang et al., 1998; Prospero et al., 2002). The most significant sources of dust are associated with the Makgadikgadi Pans in Botswana (Bryant et al., 2007) and Etosha Pan in Namibia (Figure 1; Prospero et al., 2002). These systems represent large internal drainage basins that during the Pleistocene were occupied by large lakes (Thomas and Shaw, 1991), but today receive only seasonal drainage from a network of small ephemeral rivers and streams. The fine-grained lacustrine sediment within these systems is vulnerable to aeolian entrainment and both lake basins are associated with well-defined and persistent dust plumes (Figure 1B, inset). The Makgadikgadi Pans (22 000 km^2) are considered the principal dust source in southern Africa (Prospero et al., 2002; Washington et al., 2003; Vickery et al., 2013), with dust activity centred over the western end of the pans. The dominant easterly winds in the region appear to have been a persistent feature of the Quaternary climate in the Kalahari region, as evidenced by the ENE–WSW orientation of former linear dune systems (Thomas and Shaw, 1991). A smaller, but persistent dust source is centred over Etosha Pan (4800 km^2) in northern Namibia. The dust cycles of both lake basins are identical, and during some years, satellite observations show dust activity across the entire region, extending from central Botswana to northern Namibia (Prospero et al., 2002). Combined, these two regions contribute large quantities of dust that circulate in anticyclonic systems over southern Africa (Tyson *et al.*, 1996). On a more local scale, ephemeral river valleys in Namibia have been identified as important sources of wind-erodible sediment and are associated with short-lived dust plumes that extend over the South Atlantic Ocean (Eckardt and Kuring, 2005; Vickery et al., 2013; Dansie et al., 2017).

Methods

Samples

Except for its marginal areas, the Okavango Delta is virtually unpopulated and difficult to access. The three islands selected for study are located in the seasonal swamps (Figure 1B) and are the same sites that were studied by Humphries et al. (2014). The local-scale topography of the study region is gently undulating, comprising grassland and wetland communities that are typical of the seasonal swamps. The higher-lying ground is never flooded and supports large trees near the island edges.

The islands sampled (A, C and D) were in close proximity to each other and ranged in diameter from 250 to 450 m (Figure 2). Island elevation varied from 0.5 to 2.5 m relative to the surrounding floodplain. Surface soil samples (top ~5 cm) were collected along traverses across the centre of each island, as described by Humphries et al. (2014). Ten of these samples were subsequently selected for detailed trace element and isotope analyses. Several additional samples were collected from the Okavango region and included surface material from the seasonal floodplains (n = 5), river channels (n = 5) and surrounding Kalahari Desert (n = 3). Included in our sample suite is a dust sample that was collected by Krah et al. (2004) using a passive wet dust collector deployed on the floodplain in close proximity to our study islands. This sample was analysed for its particle size and trace metal composition, but did not yield sufficient material for subsequent isotope and nutrient analyses. We also collected surface material from the two major dust emitters in southern Africa; the dry lake beds of Etosha Pan (n = 3) and the Makgadikgadi Pans (n = 3). These consisted of fine-grained, powdery sediment that contained considerable quantities of evaporite minerals, mainly calcite and halite.

Grain size analysis

The grain size distribution of samples collected from the Okavango Delta and potential dust source areas was analysed by wet dispersion using a Malvern Mastersizer. Prior to analysis, bulk samples were combusted at 550°C and then leached with 10% HCl to remove organic matter and carbonate, respectively. The resulting residue was dispersed in 5% sodium hexametaphosphate, sonicated, and analysed in triplicate.

Mineral dust is typically transported in long-term (<20 μm) and short-term (20–70 μm) suspension (Kok et al., 2012), although larger particle sizes are also susceptible to transport at local and regional scales (e.g. van der Does et al., 2018). Endmember modelling was applied to determine the proportions of distinct sediment components contributing to the measured grain size signal in island samples. Volume size distributions were fitted with log-normal functions based on the parsimony between the number of endmembers and the goodness-of-fit (Sun et al., 2002). Analyses indicated that variations in the particle size distribution of surface material from the islands could be attributed to two distinct populations; sandy coarse material (mode ~250 μm) and a fine-grained component (mode ~50 μm). In order to compare dust of equivalent size between sources and sinks, and reduce the effect of grain size on measured isotope values, all samples for subsequent isotope and chemical analysis were dry-sieved to isolate the <53 μm fraction. This size fraction was considered most appropriate for assessing regional dust deposition, given the nature of Okavango island sediments and the characteristics of deposits from Etosha and the Makgadikgadi Pans, both of which are dominated (83 and 92%, respectively) by particles finer than 53 μm. All subsequent chemical analyses were performed on the <53 μm size fraction.

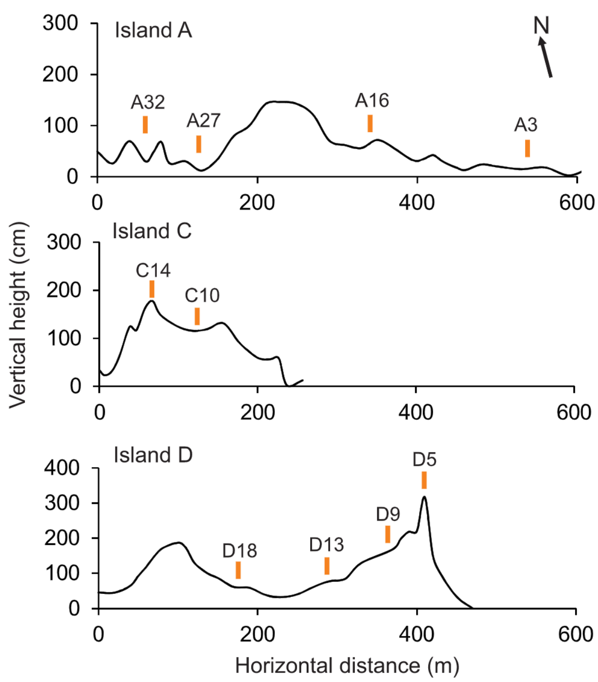

Figure 2. Topographic profiles (vertical height above the floodplain) and sampling locations and IDs for the three islands studied. [Colour figure can be viewed at wileyonlinelibrary.com]

Isotope and trace metal analyses

We employed a combination of trace metal and radiogenic isotope (Nd and Sr) tracers to characterize potential dust source areas and compare results with surface material collected from islands in the Okavango Delta. Samples were combusted at 550°C and leached with 10% HCl prior to being measured at the Center for Elemental Mass Spectrometry at the School of Earth, Ocean and Environment, University of South Carolina. Briefly, about 50 mg of sample was digested in a concentrated mixture of HF: HNO_3 for 3 days and then evaporated to dryness several times with concentrated HNO_3. One aliquot was gravimetrically separated for trace element analyses, and a second aliquot for Sr and Nd isotopes. Trace-element concentrations were determined on a THERMO ELEMENT 2, HR-ICPMS using a combination of low-, medium- and high-resolution modes to resolve isobaric interferences (e.g. $ArOH^+$ on $^{57}Fe^+$). The separated aliquots were spiked with 2 ppb In, and quantified using a combination of internal drift correction and external sample-standard bracketing against the USGS reference material BHVO-2 (Jochum et al., 2016).

Sr and Nd isotopes were determined on a THERMO NEPTUNE MC-ICPMS. Sr was isolated from the bulk sample using HNO_3 media on a Sr-spec resin. For Nd, rare earth elements (REE) were first isolated from the bulk using the TRU-spec resin and Nd was purified using 100 μl micro-columns filled with Ln resin (Frisby et al., 2016). Sr was corrected for mass fractionation using $^{86}Sr/^{89}Sr$ = 0.1194. The NBS 987 standard was determined at $^{87}Sr/^{86}Sr$ = 0.710321 ± 0.000011 (two standard deviations, n = 7), and all values are reported relative to the NBS 987 value of $^{87}Sr/^{86}Sr$ = 0.710248. Nd was corrected for mass fractionation using $^{146}Nd/^{144}Nd$ = 0.7219. The Nd reference material JNdi-1 was determined at $^{143}Nd/^{144}Nd$ = 0.512093 ± 0.000005 (two standard deviations, n = 9), and the values are reported relative to the JNdi-1 value of $^{143}Nd/^{144}Nd$ = 0.512115. ϵNd values are calculated using the chondritic ratio of $^{143}Nd/^{144}Nd$ = 0.512630.

Iron and phosphorus analyses

Nutrient limitation to primary productivity and other biological processes is widespread in terrestrial ecosystems; with phosphorus generally considered the most common limiting element, either independently or in combination with nitrogen (Newman, 1995; Vitousek *et al.*, 2010). While receiving far less attention, there is evidence to suggest that micronutrients, such as iron, can be limiting to algal growth and productivity in freshwater ecosystems (Sterner, 2008; Larson *et al.*, 2015). Iron also plays a crucial role in the nitrogen cycle through its influence on N_2 fixation. Given the nutrient-poor substrate underlying the Delta and the generally low level of chemical weathering, we focused on the supply of phosphorus and iron in assessing the importance of dustborne nutrients to the Okavango.

The bioavailability of dustborne nutrients is particularly important in evaluating potential influences on biological productivity, and various analytical extraction protocols have been employed in evaluating nutrient solubility in dust, with little consensus between individual laboratories (e.g. Anderson et al., 2010; Paris et al., 2011). We measured extractable P and Fe concentrations on pre-combusted sub-samples (250 mg) that were leached in 10 ml of 1.2 M HCl for 10 min. This acid solution extraction likely provides an upper-limit estimate of bioavailable phosphorus and iron, targeting poorly crystalline and oxyhydroxide (including goethite and hematite) iron phases (e.g. Shi et al., 2012), as well as surface-bound P, labile organic P and the acid-reactive mineral phosphate pool (e.g. Stockdale et al., 2016). Extractable Fe concentrations were measured by ICP-MS as reported above, following dilution with 2% HNO_3. Extractable P concentrations were determined using the colorimetric phosphomolybdate method developed by Koroleff (1983). To monitor run variability and validate analytical accuracy, an internal standard and a standard reference material, estuarine sediment (NIST# 1646a), were included.

Results

Grain size distributions

Island surface sediments consist of unconsolidated, brown to grey sand. The most abundant constituent in all of the samples is well-rounded quartz sand, with a mode of ~250 μm (Figure 3a). This material is texturally similar to the sand forming the dunes south of the study area (McCarthy and Ellery, 1995) and typical of the sand that blankets the entire Kalahari region (Thomas and Shaw, 1991). All island samples were characterized by a secondary mode, defined by a dominant peak at ~50 μm, reflecting varying proportions of fine-grained material.

The contribution of this fine-grained component to islands varies substantially across the range of samples examined, with the <53 μm size fraction comprising between 9 and 48% (average 21%) of surface soils. The distinctly bimodal nature of island soils contrasts with deposits that characterize the surrounding floodplains and channels of the Okavango Delta (Figure 3b), which are dominated almost exclusively by fine to medium sand, with a mode around 315 μm. Local airborne material is composed predominantly of fine-grained components (~60% <53 μm), but also contains sand-sized material that is presumably locally sourced (Figure 3b, orange colour).

Geochemical characterization

The fine lithic fraction of Okavango island samples exhibits REE patterns that are similar to one another with roughly flat patterns, typical of upper crustal rocks and sediments (Figure 4a, black colour). These samples can easily be distinguished from the fine-grained component of local Kalahari sand (Figure 4a, green colour), characterized by relatively enriched REE concentrations with somewhat heavy REE-enriched patterns. In contrast, sediments from Etosha and Makgadikgadi (Figure 4a, red and blue, respectively) show relatively lower REE concentration patterns which are reasonably similar to one another and compositionally comparable to dust from the Okavango Delta.

The REE patterns and geochemical characteristics of sediments from Okavango islands suggest that this material is likely mostly derived from mineral sources; a local component characterized by relatively high REE compositions (Kalahari sand) and a more distal, REE-depleted component (dust from Etosha and/or Makgadikgadi) (Figure 4b).

Isotopic compositions

The Sr–Nd isotopic ratios measured in samples from the Okavango Delta and potential dust sources are reported in Table I and shown in Figure 5a. Okavango islands are characterized by variable Sr isotopic compositions, ranging between 0.726 and 0.761 (Table S1), and rather unradiogenic Nd values (ϵNd), ranging from −22.1 to −17.7. These samples are clearly separated from the fine material carried by channels on the fan ($p < 0.01$), which occupy a relatively narrow $^{87}Sr/^{86}Sr$ range (0.720 to 0.732) and display on average slightly lower Nd values (ϵNd = −21.5 ± 0.7). Sediments from Etosha and Makgadikgadi Pans are characterized by very similar isotopic compositions (ϵNd = −20 to −15; $^{87}Sr/^{86}Sr$ = 0.722 to 0.724) and together define a distinct field that can easily be distinguished from Namib Desert dust, which exhibits relatively

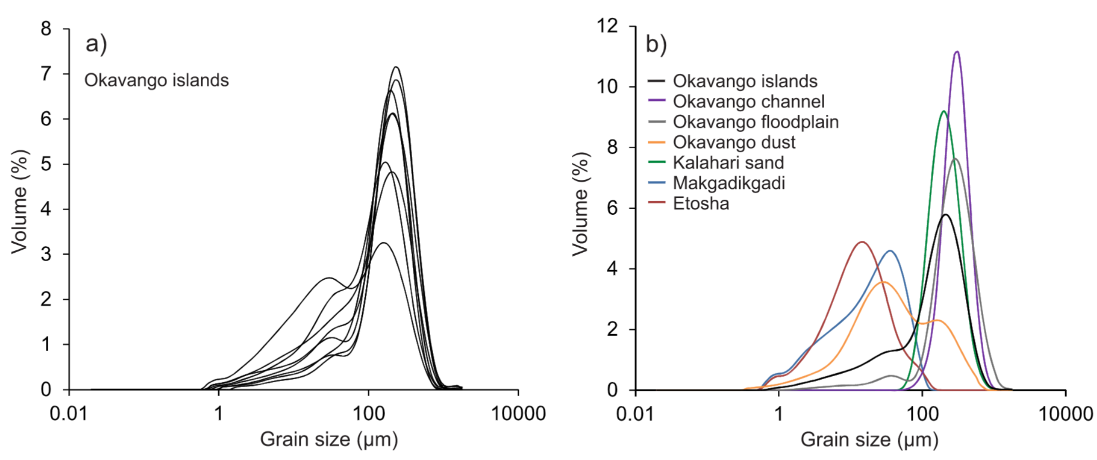

Figure 3. Grain size distributions. (a) Variation in grain size distribution of surface material from Okavango islands. (b) Average grain size distributions of sediment from potential source areas and different environments in the Okavango. [Colour figure can be viewed at wileyonlinelibrary.com]

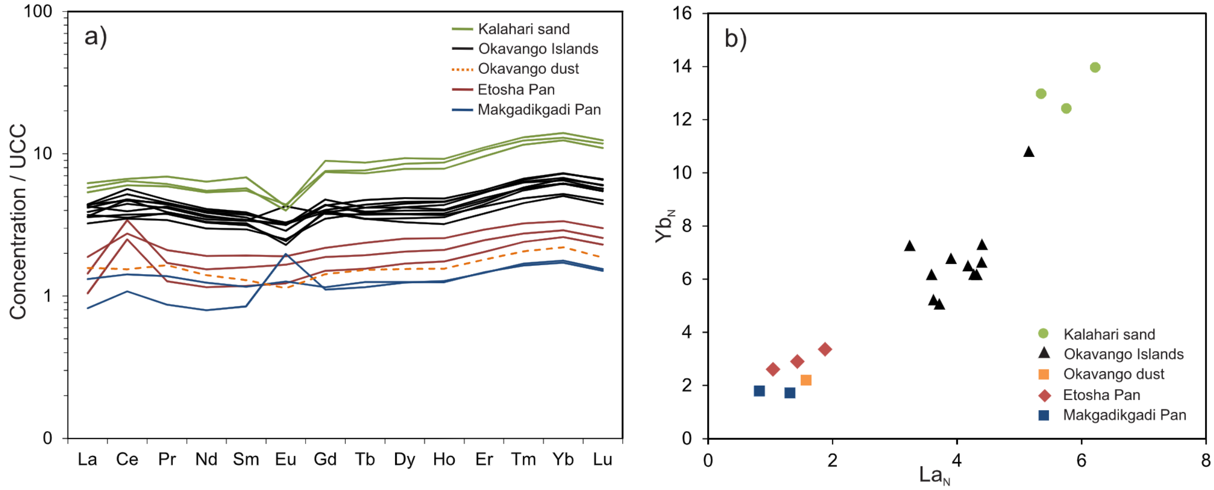

Figure 4. (a) Normalized REE patterns. (b) Variation in normalized La vs. Yb concentrations in the <53 µm fraction of Okavango island sediments and potential sediment sources. REE concentrations are normalized to average continental crust concentration (Wedepohl, 1995). [Colour figure can be viewed at wileyonlinelibrary.com]

Table I. Sample locations and Sr–Nd isotopic data

Sample site	Sample type	Location (latitude, longitude)	$^{87}Sr/^{86}Sr$ ($\pm 2\sigma \times 10^{-6}$)	$^{143}Nd/^{144}Nd$ ($\pm 2\sigma \times 10^{-6}$)	εNd	Nd/Sr
Okavango Delta, Botswana						
A3	Island soil	19.546 S, 23.179 E	0.746397 (±12)	0.511624 (±4)	−19.7	0.236
A16	Island soil	19.545 S, 23.177 E	0.756542 (±9)	0.511553 (±6)	−21.1	0.286
A27	Island soil	19.544 S, 23.175 E	0.741072 (±8)	0.511596 (±4)	−20.3	0.176
A32	Island soil	19.544 S, 23.174 E	0.760804 (±7)	0.511601 (±6)	−20.2	0.248
C10	Island soil	19.548 S, 23.169 E	0.733193 (±6)	0.511611 (±4)	−20.0	0.125
C14	Island soil	19.548 S, 23.168 E	0.736160 (±6)	0.511627 (±6)	−19.7	0.119
D5	Island soil	19.533 S, 23.153 E	0.726927 (±6)	0.511723 (±8)	−17.8	0.049
D9	Island soil	19.533 S, 23.152 E	0.738025 (±7)	0.511554 (±6)	−21.1	0.159
D13	Island soil	19.533 S, 23.151 E	0.757604 (±7)	0.511499 (±6)	−22.2	0.215
D18	Island soil	19.532 S, 23.150 E	0.726285 (±5)	0.511622 (±6)	−19.8	0.206
Makgadikgadi Pans, Botswana						
MP1	Lake sediment	21.026 S, 25.622 E	0.722589 (±7)	0.511854 (±4)	−15.3	0.116
MP2	Lake sediment	20.940 S, 25.660 E	0.724464 (±7)	0.511787 (±6)	−16.6	0.013
MP3	Lake sediment	20.805 S, 25.701 E	0.722603 (±8)	0.511780 (±4)	−16.7	0.031
Kalahari, Botswana						
MP7	Aeolian sand	21.722 S, 21.650 E	0.756648 (±6)	0.511826 (±6)	−15.8	0.247
MP8	Aeolian sand	23.698 S, 22.814 E	0.745008 (±6)	0.511942 (±6)	−13.5	0.464
Etosha Pan, Namibia						
ET1	Surface crust	18.929 S, 16.488 E	0.722898 (±8)	0.511800 (±5)	−16.3	0.045
ET2	Lake sediment	18.930 S, 16.487 E	0.721209 (±8)	0.511673 (±5)	−18.8	0.036
ET5	Lake sediment	18.929 S, 16.488 E	0.721844 (±6)	0.511595 (±7)	−20.3	0.028

radiogenic Nd values (εNd = −13 to −4). The signature of Kalahari sediment is not well constrained, with these samples showing extremely variable Sr and Nd isotopic ratios (Figure 5a). The marked variability in composition likely reflects the geological variability of the Kalahari Basin and the wide area from which the limited number of samples (n = 3) were collected. Although we are not able to fully characterize the Kalahari dust isotopic signature, these samples carry relatively high radiogenic $^{87}Sr/^{86}Sr$ ratios (~0.75 to 0.78; Figure 5a) which are distinct from the Okavango and pan samples. The wide range of isotopic composition exhibited by Okavango island samples supports the REE data and suggests mixing between at least two isotopically distinct endmembers; a relatively radiogenic Sr source (Kalahari sand) with a significantly less radiogenic Sr component (Figure 5b). Notably, Kalahari sands are typified by unusually high Nd/Sr ratios that are markedly different ($p < 0.001$) from those characteristic of material from Etosha and the Makgadikgadi Pans (Figure 5b). Okavango island samples fall along a trend between these two isotopically distinct sources and are clearly distinguishable from the fine-grained material that characterizes Okavango channels.

Phosphorous and iron concentrations

The fine fraction of sediments from the Okavango islands was characterized by highly variable quantities of extractable Fe and P (Figure 6). Extractable Fe concentrations varied between 170 and 3000 ppm (809 ± 897 ppm), with most samples containing less than 500 ppm. Extractable P varied between 9.4 and 268 ppm, and was on average around an order of magnitude lower (82.3 ± 86.8 ppm) than iron concentrations. While the majority of island sediments were characterized by

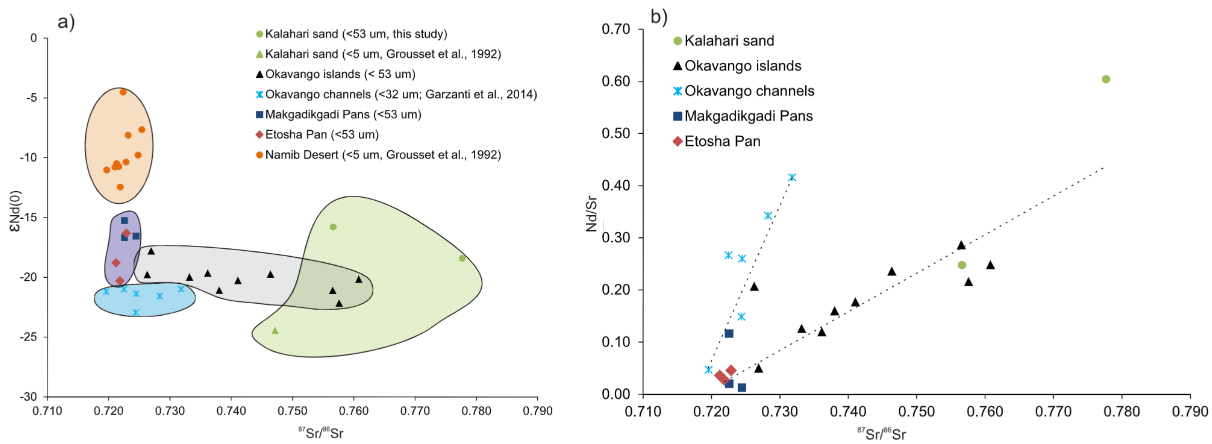

Figure 5. (a) $^{87}Sr/^{86}Sr$ vs. Nd isotopic signature of Okavango island soils in relation to possible local and regional sources. Isotopic field lines are outlined based on the available points. (b) $^{87}Sr/^{86}Sr$ vs. Nd/Sr. Note that the composition of Okavango island samples falls along an array that is consistent with mixing between an unradiogenic Sr endmember and a radiogenic Sr endmember. The fine-grained material on islands is chemically distinct from that found in Okavango channels. [Colour figure can be viewed at wileyonlinelibrary.com]

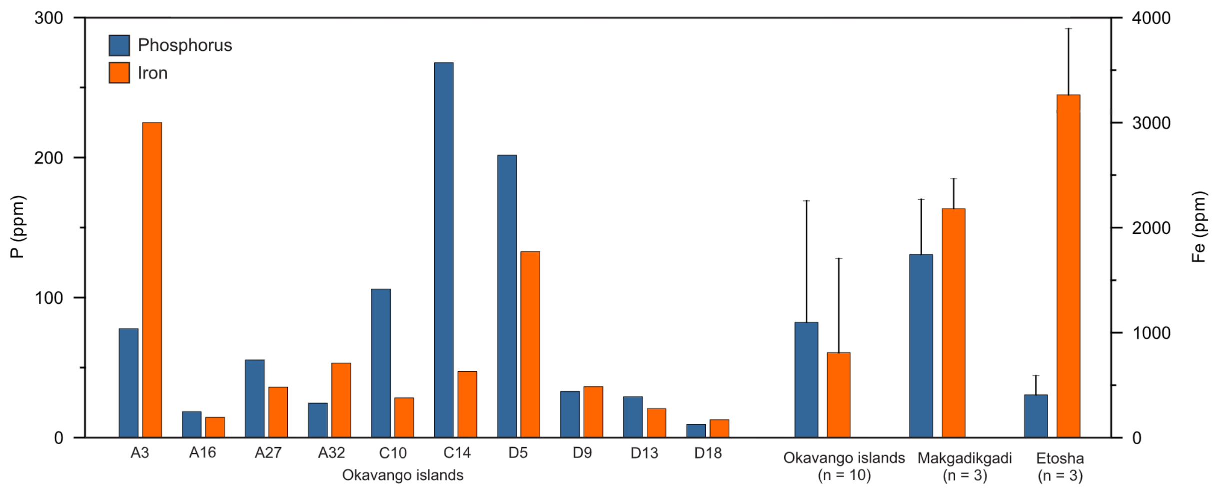

Figure 6. Extractable phosphorus and iron in the <53 μm fraction of surface sediments from Okavango islands and key southern African dust sources. All data provided in Table S1 (see Supporting Information). [Colour figure can be viewed at wileyonlinelibrary.com]

extractable P concentrations lower than 100 ppm, samples C14 and D5 (from the topographically highest collection points) were significantly enriched ($p < 0.05$), containing 268 and 202 ppm, respectively. There was no correlation ($R^2 < 0.1$) between extractable Fe and P concentrations in the island samples.

In comparison to Okavango island sediments, surficial material from Etosha and Makgadikgadi Pans was relatively enriched in extractable Fe, containing 2181 ± 283 and 3625 ± 630 ppm, respectively. Pan sediments were also enriched in extractable P, although the Makgadikgadi Pans (131 ± 39.4 ppm) contained significantly higher concentrations compared to Etosha samples (31 ± 13.7 ppm).

Discussion

Provenance of fine-grained material on Okavango islands

Sediments from islands in the Okavango exhibit particle size distributions that are distinctly different from that of the surrounding landscape, indicating that the fine material present in island soil likely has an external origin. A distal supply of fine material is supported by variations in trace metal and isotope compositions, which suggest that Okavango island soils result from mixing between two isotopically distinct sources. Based on the suite of samples analysed here, our data suggest that locally derived Kalahari material provides a likely source of radiogenic Sr, while aeolian material deflated from Etosha and/or the Makgadikgadi Pans provides a potential source of unradiogenic Sr (Figure 5a). The grouping of the Okavango island isotopic data between these endmembers implies that the Nd–Sr signatures of island sediments can be explained by simple mixing from two primary sources; one local and one regional (Figure 5b).

To calculate the relative contribution of dust to island soils, we employed a two-component mixing model (Figure 7a). For this calculation, we used the mean isotopic composition of sediment from the Makgadikgadi Pans to represent the distal endmember. Surface sediments from Makgadikgadi and Etosha Pans are indistinguishable based on their Nd–Sr isotope and trace metal composition, however we consider emissions from the Makgadikgadi Pans to be the overwhelming source of regional dust to the Okavango based on satellite observations of

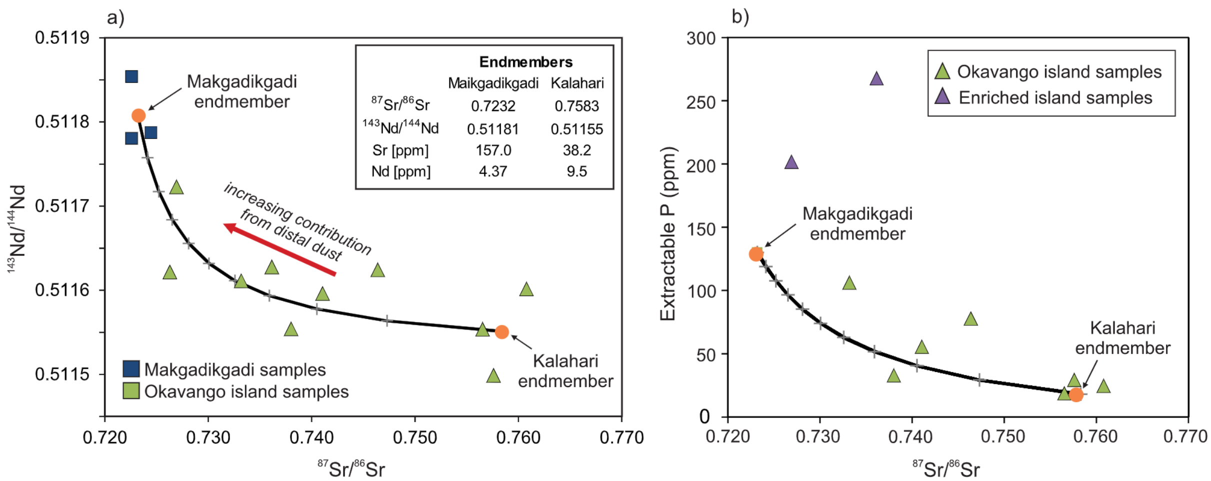

Figure 7. (a) Sr–Nd binary mixing model. The solid black line represents a modelled mixing curve between the two hypothesized sources of sediment to islands in the Okavango. This model suggests that Sr isotopic signatures of island samples can be produced by a simple mixing of Kalahari sediment with variable proportions of dust from the Makgadikgadi Pans. Tick marks along the mixing curve indicate 10% intervals. Also shown are the compositions of the endmembers used in the mixing model. (b) Binary mixing model applied to measured concentrations of extractable phosphorus in Okavango island samples. The mixing array suggests that variability in extractable phosphorus may be explained by variations in the proportion of Makgadikgadi dust. [Colour figure can be viewed at wileyonlinelibrary.com]

dust activity in the region (Prospero et al., 2002; Vickery et al., 2013). The dominant wind direction favours westerly transport from the Makgadikgadi Pans that are close in geographic proximity to the Delta versus the Etosha Pans that are located further away to the west. Pinpointing the composition of the local endmember is more difficult given the variability in composition of Kalahari sediment across the region. We estimated the composition of this endmember using an average of the most radiogenic Sr island samples (n = 3). These samples fall within the Kalahari isotopic field and therefore likely provide a good indication of the locally sourced material.

The model reveals that regional dust contributes between ~10 and 80% of the fine-grained component of Okavango island sediments. The contribution of regional dust to sediments also appears to vary systematically across the surface of islands, with samples from the island interiors (C10, D18) and tree-lined fringes (C14, D5) characterized by relatively higher proportions of distal dust compared to those collected from nearer the floodplain edge (A3, A16, A32). Although our data are limited, this pattern of variation suggests that local-scale topographic and vegetation differences across the surface of islands causes dust to preferentially concentrate on these elevated sites. This is consistent with Krah et al. (2004), who found dust loads in the seasonal swamps of the Okavango to be highest on floodplains and lowest over the interior of islands. Whilst floodplains are broad, open areas that facilitate the aeolian redistribution of fine material, trees in the riparian fringes around islands substantially impede the movement of air, trapping airborne material.

Potential nutrient inputs from windblown dust

Our isotopic results confirm that islands in the Okavango are sites of regional dust accumulation. This dust constitutes a major component of the fine-grained material found in island soils and may therefore play a significant role in mediating biogeochemical processes in the nutrient-poor, sandy soils of the Okavango. Local Kalahari sediments, including the fine-grained fraction, are composed almost entirely of pure quartz (Wang et al., 2007). These soils are thus extremely nutrient-poor and plant growth in the Kalahari is considered to be P-limited, with a tight seasonal coupling observed between plant growth and soil phosphate concentrations (Wang et al., 2009). In contrast to the nutrient-starved landscape of the Kalahari, fine sediments accumulated in Etosha and the Makgadikgadi Pans provide pockets of relatively nutrient-rich material. These basin systems receive inflow from rivers that drain wetter regions farther north; Etosha Pan drains the inland interior of northern Namibia and southern Angola (Miller et al., 2010), while the primary inflow into the Makgadikgadi Pans is via the ephemeral Nata River and other smaller, intermittently flowing streams that drain the eastern regions of Zimbabwe (Figure 1A; Thomas and Shaw, 1991). These streams likely support corridors of biological productivity, providing transport pathways that deliver fine sediment and nutrients to the lake basins during flood events.

We show that deflatable material from Etosha and the Makgadikgadi Pans contains relatively high amounts of extractable Fe and P (Figure 6). Makgadikgadi is especially rich in both total phosphorus (TP = ~500 ppm; Bhattachan et al., 2015) and bioavailable P (~130 ppm) compared to sediments from Etosha (TP = ~150 ppm, bioavailable P = ~30 ppm). Marked differences in P content between the two basins likely reflect inherent variations in their catchment area. The Makgadikgadi Pans are also known to attract flamingos, which congregate in high densities during the breeding season (McCulloch and Borello, 2000). Flamingo faeces are especially rich in nitrogen and phosphorus (Batanero et al., 2017), and likely represent an important source of additional nutrients. The notable differences in P content between Etosha and Makgadikgadi relative to P concentrations measured in Okavango island soils support our isotopic data and suggest that the Makgadikgadi Pans are the most likely regional source of dust to the Okavango.

To estimate the proportion of bioavailable P present in Makgadikgadi sediments, we use TP values reported by Bhattachan et al. (2015), although we note that these measurements were performed for <45 μm, which differs slightly from that employed in this study. Based on an average TP value of 500 ppm, we find that approximately 25% of the total phosphorus present in Makgadikgadi sediments is extractable and thus potentially available for biological uptake. To investigate this further, we applied the two-component mixing model developed using Nd and Sr isotopes (Figure 7a) to the extractable P concentrations measured in island soils. Here, we considered mineral dust from the Makgadikgadi Pans to be the dominant supply of bioavailable P to Okavango islands. One potentially important source of P that we are unable to capture in our mixing model is biomass burning emissions (Mahowald *et al.*, 2005; Wang et al., 2014). Savanna fires dominate the tropical and equatorial region of Africa, and each year biomass burning aerosols emitted during the fire season (July–October) are transported westward over the southeast Atlantic Ocean (Sinha et al., 2003; Liousse et al., 2010; Bauer et al., 2019). Botswana has comparatively low quantities of biomass and contributes little to the total amount of fuel burned in open vegetation fires in southern Africa (Roberts et al., 2009). Nevertheless, elevated seasonal concentrations (150–550 ppbv) of CO, substantially greater than those typical of remote regions (50–150 ppbv), have been measured over Botswana (Sinha et al., 2003) and are hypothesized to reflect the transport of emissions into Botswana from surrounding regions where intense biomass burning occurs (e.g. Zambia and Angola). However, there remain large uncertainties inherent in the determination of biomass burning emission inventories (e.g. Shi et al., 2015) and the particulate material emitted, with some studies showing African savanna fire emissions to be a negligible source of P (Cachier et al., 1995; Maenhaut et al., 1996). While we cannot evaluate the potential contribution of biomass burning to P deposition, we consider mineral dust, which dominates the aerosol load in the region, to likely be the principal source of atmospheric P to the Okavango Delta.

Bearing in mind these limitations to our modelling approach, the results show that mixing between the two hypothesized endmembers largely explains the variability in concentrations, with bioavailable P becoming progressively enriched in island soils that contain increasing proportions of Makgadikgadi-sourced dust (Figure 7b). Notably, two island samples (C14 and D5) showed pronounced enrichment in bioavailable P, exceeding that of the Makgadikgadi endmember. These samples are both substantially elevated relative to the other samples and are associated with large tree-covered termite mounds. In the Okavango, termites commonly forage on the floodplain for leaf litter, grass and mammalian (especially elephant) dung (McCarthy et al., 1998), resulting in the redistribution and local enrichment of nutrients in mounds. Large termite mounds in the Okavango have thus been identified as sites of nutrient concentration, particularly for P and potassium (McCarthy et al., 1998). Trees, which become established on this higher-lying ground, also likely contribute to the recycling of phosphorus through litterfall. The higher concentrations of bioavailable P measured in these samples are thus not surprising considering their location.

The lack of correlation between bioavailable P and Fe concentrations suggests that Fe in island soils is likely not derived exclusively from atmospheric deposition. When compared to P concentrations, Kalahari (2.2 ± 0.33%) and Okavango island (1.61 ± 0.71%) sediments contain relatively high amounts of iron. However, the majority of this iron is associated with iron oxides and largely not bioavailable (Bhattachan et al., 2015; Dansie et al., 2017), with extractable iron in Okavango island soils comprising a very small proportion (3.8 ± 2.3%) of total iron concentrations. In contrast, approximately 20% of the iron present in Makgadikgadi sediments is extractable. Thus, while Makgadikgadi-derived dust is not the only source of Fe in the Okavango, dust inputs likely represent an important supply of bioavailable Fe to the ecosystem.

Assessing the contribution of atmospheric nutrient deposition to nutrient budgets in the Okavango Delta is complex, as different sub-habitats are characterized by their own nutrient pools and fluxes, and data are limited. Although water in the Okavango Delta is characterized by extremely low nutrient concentrations, P introduced onto the floodplains by seasonal flooding may be assimilated by plants and incorporated into biomass. Floodplain vegetation is composed largely of sedge (*Cyperus articulatus*) and grass (*Imperata*) species, with biomass typically varying between 200 and 400 g DW m^{-2} (Ramberg et al., 2010). Due to strong annual shifts in the distribution of water, the seasonal floodplains in the southern reaches of the Okavango Delta are susceptible to burning during the dry season (from May to September) and commonly experience burning every 3 to 5 years (Heinl et al., 2007; Ramberg et al., 2010). Nutrients stored in floodplain biomass thus represent a potential local source of atmospheric P to islands, although the P content of plant material found on the seasonal floodplains of the Okavango Delta is low, varying between 3.4 and 6.0 ppm (Ramberg et al., 2010). Peat fires are also common in the Okavango Delta, which typically develop in wetlands adjacent to abandoned channels (Gumbricht et al., 2002). These events produce low-intensity, smouldering fires that may last for several years. Given the nutrient-poor, low biomass production on floodplains, we hypothesize that local biomass burning is not a dominant process contributing to atmospheric P deposition on tree island ecosystems in the Okavango. This is partly supported by the particle size distribution characteristics of island soils. The emission of particulate matter during biomass burning occurs mainly in the form of sub-micrometre particles (Crutzen and Andreae, 1990), which cannot account for the bulk of the fine-grained material found in island soils. We note, however, that soil dust may be entrained during fire events and contribute to atmospheric P loadings. Uncertainties regarding potential contributions from biomass burning emissions hamper our ability to be definitive about the sources of atmospheric P to the Okavango Delta, and are worthy of further work.

Islands of fertility in the Okavango Delta

Using a dust deposition rate of 250 000 tonnes per annum (Garstang et al., 1998) and an average island bioavailable P concentration of 0.044 ± 0.03 mg g^{-1}, we estimate that the Okavango Delta receives 11 000 ± 7500 kg of bioavailable P each year. This suggests that airborne dust may play an important role in supplying bioavailable P to the Okavango Delta, although the relative contribution of this source is likely to vary both temporally and spatially. It is estimated that between 60 and 600 tonnes of P is introduced onto the Delta by water inflow (Garstang et al., 1998). While data to quantify nutrient pools and fluxes associated with different sub-habitats within the Okavango ecosystem are lacking, water inflow likely represents the dominant source of nutrients to the channel fringe areas of the permanent swamps. On the seasonal floodplains and distal areas of the Delta, atmospheric sources likely play a more important and possibly dominant role in nutrient supply. Seasonal floods may contribute nutrients to the soils during the wet season, although the nutrient content and particulate load of this hydrological flow are likely to be further reduced as it moves through the channel margins of the permanent swamps. While the relative contribution of inflowing water and dust fallout to overall nutrient stocks on the floodplains is difficult to determine, surface soils on tree islands are not subjected to annual flooding. These elevated sites display higher concentrations of bioavailable P compared to floodplain soils, which we suggest is strongly controlled by dust deposition. We propose that the islands in the Okavango are nutrient-rich 'hot spots' in the landscape and serve as important fertilization sites. Assuming that all the available P is used and using a C: P ratio of 48: 1 for the Okavango (Lindholm et al., 2007), we calculate potential new primary production resulting from atmospheric deposition to be on the order of 528 000 kg C a^{-1}.

Compared to the seasonally inundated grasslands on the floodplain, islands are characterized by a greater diversity of plants and the accumulation of nutrient-loaded dust on islands likely allows plants requiring nutrient-rich soil (e.g. *Cynodon dactylon*) to thrive on islands (Garstang et al., 1998). These plants in turn support a productive and diverse ecosystem, with islands playing a potentially important role in shaping animal foraging patterns. Vegetation growing on islands has a high forage quality (Garstang et al., 1998), and therefore attracts a wide variety of bird and mammal species. Islands in the Okavango are commonly foraged by aardvark, warthogs, rodents and mongoose, while mega-herbivores (elephant, rhino and giraffe) have a particular preference for woody plant species growing on islands (McCarthy et al., 1998). Indeed, preferential browsing and grazing by large herbivores on termite-mound vegetation has been observed in numerous African savannas (Grant and Scholes, 2006; Levick et al., 2010; Seymour et al., 2014). We recognize that animal utilization of islands in the Okavango may also contribute to the nutrient status of island soils through leaf litter and dung input. However, animals also export island nutrients as well. On the Okavango fan, birds and elephants are likely the main agents of dispersal and elephants have been observed to move between large islands in search of food during the dry season (McCarthy et al., 1998). In an otherwise nutrient-starved environment, the enrichment of dustborne nutrients on islands may thus regulate dynamic feedback between biota and the physical environment.

Conclusions

Our results show that regional dust forms an important component of island sediments and may play a role in sustaining the diverse Okavango ecosystem. The majority of this dust appears to originate from the Makgadikgadi Pans and represents a significant source of bioavailable phosphorus and iron to the Okavango Delta. In an environment where productivity is constrained by the availability of nutrients, the supply of dustborne nutrients likely plays a significant role in mediating biogeochemical processes and governing biological productivity, as has been demonstrated in other nutrient-limited environments (Chadwick et al., 1999; Davidson et al., 2004). While we cannot evaluate the potential contribution of biomass burning emissions to our measured P values, mineral aerosols appear to be an important, if not dominant, source of P input to tree island ecosystems. Our findings highlight the importance of aeolian processes in not only supplying nutrients to the Okavango, but also creating islands of fertility through the redistribution of nutrient-loaded dust within the surrounding seasonal floodplains.

The contribution of dustborne nutrient inputs to the Okavango is likely to vary in relation to dust emission and deposition rates, which may be dramatically impacted by changes in climate (e.g. Okin and Reheis, 2002). Annual and interannual variability in dust emissions from the Makgadikgadi Basin has been shown to be significantly influenced by the extent and frequency of lake inundation, which exerts a primary control on sediment availability for deflation (Bryant et al., 2007). Inundation events are strongly associated with the El Niño Southern Oscillation (ENSO) and Indian Ocean sea surface temperature anomalies, with reduced precipitation during El Niño contributing to the increased frequency of dust events in the region (Bryant et al., 2007). Variations in dust deposition and nutrient cycling in the Okavango may thus be sensitive to changes in climate, and in particular the magnitude and frequency of extreme events associated with ENSO cycles, which are expected to increase in response to future global warming (Cai et al., 2013). While the actual influence of dust in maintaining productivity in the Okavango remains unknown, our results indicate that the contribution of airborne nutrients to the functioning of the ecosystem cannot be ignored. Given the prominent role that dustborne nutrients likely play in the nutrient budget of the Okavango Delta, understanding the relationship between dust deposition, nutrient loads and biogeochemical cycling requires further attention, particularly in predicting the response of the Okavango ecosystem to future changes in climate. While the Okavango Delta is a unique system, dust fallout is likely to play an important, but so far understudied, role in sustaining the productivity of other wetland systems located in dryland environments, including those found in southern Africa, Australia and South America.

Acknowledgements—This study did not receive any direct funding, but benefitted from discretionary funds provided by the University of the Witwatersrand, a South African National Research Foundation Grant to MSH (105724) and a Macquarie University Research and Development Grant to TJR. Wayne Buckley is thanked for his assistance with the trace element and isotope analyses. Martin Krah, Richard Stewart and Clinton Wreghitt assisted in the collection of samples.

Data Availability Statement

The data that support the findings of this study are available in the Supporting Information for this article.

Conflict of Interest Statement

The authors declare no conflict of interest.

References

Aciego SM, Riebe CS, Hart SC, Blakowski MA, Carey CJ, Aarons SM, Dove NC, Notthoff JK, Sims KWW, Aronson EL. 2017. Dust outpaces bedrock in nutrient supply to montane forest ecosystems. *Nature Communications* **8**: 14800. https://orcid.org/10.1038/ncomms14800

Allan JR, Kormos C, Jaeger T, Venter O, Bertzky B, Shi Y, Mackey B, van Merm R, Osipova E, Watson JEM. 2017. Gaps and opportunities for the World Heritage Convention to contribute to global wilderness conservation. *Conservation Biology* **32**: 116–126.

Anderson LD, Faul KL, Paytan A. 2010. Phosphorus associations in aerosols: what can they tell us about P bioavailability? *Marine Chemistry* **120**: 44–56.

Batanero GL, León-Palmero E, Li L, Green AJ, Rendón-Martos M, Suttle CA, Reche I. 2017. Flamingos and drought as drivers of nutrients and microbial dynamics in a saline lake. *Scientific Reports* **7**: 12173. https://orcid.org/10.1038/s41598-017-12462-9

Bauer SE, Im U, Mezuman K, Gao CY. 2019. Desert dust, industrialization, and agricultural fires: health impacts of outdoor air pollution in Africa. *Journal of Geophysical Research: Atmospheres* **124**: 4104–4120.

Bhattachan A, D'Odorico P, Okin GS. 2015. Biogeochemistry of dust sources in Southern Africa. *Journal of Arid Environments* **117**: 18–27.

Bristow CS, Hudson-Edwards KA, Chappell A. 2010. Fertilizing the Amazon and equatorial Atlantic with West African dust. *Geophysical Research Letters* **37**: L14807. https://orcid.org/10.1029/2010GL043486

Bryant RG, Bigg GR, Mahowald NM, Eckardt FD, Ross SG. 2007. Dust emission response to climate in southern Africa. *Journal of Geophysical Research* **112**: D09207. https://orcid.org/10.1029/2005JD007025

Cachier H, Liousse C, Buat-menard P, Gaudichet A. 1995. Particulate content of savanna fire emissions. *Journal of Atmospheric Chemistry* **22**: 123–148.

Cai W, Zheng X-Z, Weller E, Collins M, Cowan T, Lengaigne M, Yu W, Yamagata T. 2013. Projected response of the Indian Ocean Dipole to greenhouse warming. *Nature Geoscience* **6**: 999–1007.

Chadwick OA, Derry LA, Vitousek PM, Heubert BJ, Hedin LO. 1999. Changing sources of nutrients during four million years of ecosystem development. *Nature* **397**: 491–496.

Crutzen PJ, Andreae MO. 1990. Biomass burning in the tropics: impact on atmospheric chemistry and biogeochemical cycles. *Science* **250**: 1669–1678.

Dansie AP, Wiggs GFS, Thomas DSG. 2017. Iron and nutrient content of wind-erodible sediment in the ephemeral river valleys of Namibia. *Geomorphology* **290**: 335–346.

Davidson EA, Carvalho C, Viera I, Figueriedo R, Moutinho P, Ishida F, Santos M, Guerrero J, Kalif K, Saba R. 2004. Nutrient limitation of biomass growth in a tropical secondary forest: early results of a nitrogen and phosphorus amendment experiment. *Ecology Applications* **14**: S150–S163.

van der Does M, Knippertz P, Zschenderlein P, Harrison RG, Stuut J-BW. 2018. The mysterious long-range transport of giant mineral dust particles. *Science Advances* **4**: eaau2768. https://orcid.org/10.1126/sciadv.aau2768

Eckardt FD, Kuring N. 2005. SeaWiFS identifies dust sources in the Namib Desert. *International Journal of Remote Sensing* **26**: 4159–4167.

Ellery WN, Ellery K, Mccarthy TS. 1993. Plant distribution in islands of the Okavango Delta, Botswana: determinants and feedback interactions. *African Journal of Ecology* **31**: 118–134.

Frisby C, Bizimis M, Mallick S. 2016. Seawater-derived rare earth element addition to abyssal peridotites during serpentinization. *Lithos* **248–251**: 432–454.

Garstang M, Ellery WN, e, Scholes MC, Swap RJ, Tyson PD. 1998. The contribution of aerosol- and water-borne nutrients to the functioning of the Okavango Delta ecosystem, Botswana. *South African Journal of Science* **94**: 223–229.

Garzanti E, Padoan M, Setti M, López-Galindo A, Villa IM. 2014. Provenance versus weathering control on the composition of tropical river mud (southern Africa). *Chemical Geology* **366**: 61–74.

Grant CC, Scholes MC. 2006. The importance of nutrient hot-spots in the conservation and management of large wild mammalian herbivores in semi-arid savannas. *Biological Conservation* **130**: 426–437.

Grousset FE, Biscaye PE, Revel M, Petit J-R, Pye K, Joussaume S, Jouzel J. 1992. Antarctic (Dome C) ice-core dust at 18 k.y. B.P.: isotopic constraints on origins. *Earth and Planetary Science Letters* **111**: 175–182.

Gumbricht T, McCarthy TS, McCarthy J, Roy D, Frost PE, Wessels K. 2002. Remote sensing to detect sub-surface peat fires and peat fire scars in the Okavango Delta, Botswana. *South African Journal of Science* **98**: 351–358.

Gumbricht T, McCarthy J, McCarthy TS. 2004. Channels, wetlands and islands in the Okavango Delta, Botswana, and their relation to hydrological and sedimentological processes. *Earth Surface Processes and Landforms* **29**: 15–29.

Heinl M, Frost P, Vanderpost C, Sliva J. 2007. Fire activity on drylands and floodplains in the southern Okavango Delta, Botswana. *Journal of Arid Environments* **68**: 77–87.

Humphries MS, McCarthy TS, Cooper GRJ, Stewart RA, Stewart RD. 2014. The role of airborne dust in the growth of tree islands in the Okavango Delta, Botswana. *Geomorphology* **206**: 307–317.

Jickells TD. 1999. The inputs of dust derived elements to the Sargasso Sea; a synthesis. *Marine Chemistry* **68**: 5–14.

Jochum KP, Weis U, Schwager B, Stoll B, Wilson SA, Haug GH, Andreae MO, Enzweiler J. 2016. Reference values following ISO guidelines for frequently requested rock reference materials. *Geostandards and Geoanalytical Research* **40**: 333–350.

Junk W, Brown M, Campbell IC, Finlayson M, Gopal B, Ramberg L, Warner BG. 2006. The comparative biodiversity of seven globally important wetlands: a synthesis. *Aquatic Sciences* **68**: 400–414.

Kok JF, Parteli EJR, Michaels TI, Karam DB. 2012. The physics of wind-blown sand and dust. *Reports on Progress in Physics* **75**: 106901. https://orcid.org/10.1088/0034-4885/75/10/106901

Koroleff FI. 1983. Determination of phosphorus. Chemistry of the element in sea water. In *Sea Water Analysis*, Grasshoff K, Ehrhardt M, Kremling K (eds). Verlag-Chemie: Weinheim; 125–139.

Krah M, McCarthy TS, Annegarn H, Ramberg L. 2004. Airborne dust deposition in the Okavango Delta, Botswana, and its impact on landforms. *Earth Surface Processes and Landforms* **29**: 565–577.

Krah M, McCarthy TS, Huntsman-Mapila P, Wolski P, Annegarn H, Sethebe K. 2006. Nutrient budget in the seasonal wetland of the Okavango Delta, Botswana. *Wetlands Ecology and Management* **14**: 253–267.

Larson CA, Liu H, Passy SI. 2015. Iron supply constrains producer communities in stream ecosystems. *FEMS Microbiology Ecology* **91**: fiv041.

Levick SR, Asner GP, Kennedy-Bowdon T, Knapp DE. 2010. The spatial extent of termite influences on herbivore browsing in an African savanna. *Biological Conservation* **143**: 2462–2467.

Lindholm M, Hessen DO, Mosepele K, Wolski P. 2007. Food webs and energy fluxes on a seasonal floodplain: the influence of flood size. *Wetlands* **27**: 775–784.

Liousse C, Guillaume B, Grégoire JM, Mallet M, Galy C, Pont V, Akpo A, Bedou M, Castéra P, Dungall L, Gardrat E, Granier C, Konaré A, Malavelle F, Mariscal A, Mieville A, Rosset R, Serça D, Solmon F, Tummon F, Assamoi E, Yoboué V, Van Velthoven P. 2010. Updated African biomass burning emission inventories in the framework of the AMMA-IDAF program, with an evaluation of combustion aerosols. *Atmospheric Chemistry and Physics* **10**: 9631–9646.

Maenhaut W, Salma I, Cafmeyer J, Annegarn HJ, Andreae MO. 1996. Regional atmospheric aerosol composition and sources in the eastern Transvaal, South Africa, and impact of biomass burning. *Journal of Geophysical Research* **10**: 23631–23650.

Mahowald NM, Artaxo P, Baker AR, Jickells TD, Okin GS, Randerson JT, Townsend AR. 2005. Impacts of biomass burning emissions and land use changes on Amazonian atmospheric phosphorus cycling and deposition. *Global Biogeochemical Cycles* **19**: GB4030. https://orcid.org/10.1029/2005GB002541

McCarthy TS. 2006. Groundwater in the wetlands of the Okavango Delta and its contribution to the structure and function of the ecosystem. *Journal of Hydrology* **320**: 264–282.

McCarthy TS. 2013. The Okavango Delta and its place in the geomorphological evolution of southern Africa. *South African Journal of Geology* **116**: 1–56.

McCarthy TS, Ellery WN. 1995. Sedimentation on the distal reaches of the Okavango Fan, Botswana, and its bearing on calcrete and silcrete (Ganister) formation. *Journal of Sedimentary Research* **A65**: 77–90.

McCarthy TS, Stanistreet IG, Cairncross B. 1991. The sedimentary dynamics of active fluvial channels on the Okavango fan, Botswana. *Sedimentology* **38**: 471–487.

McCarthy TS, Ellery WN, Dangerfield JM. 1998. The role of biota in the initiation and growth of islands on the floodplain of the Okavango Alluvial Fan, Botswana. *Earth Surface Processes and Landforms* **23**: 291–316.

McCarthy TS, Humphries MS, Mahomed I, Le Roux P, Verhagen BT. 2012. Island forming processes in the Okavango Delta, Botswana. *Geomorphology* **179**: 249–257.

McCulloch GP, Borello W. 2000. The importance of the Makgadikgadi salt pans in Botswana for flamingos in Africa. *Waterbirds: The International Journal of Waterbird Biology* **23**: 64–68.

Miller R, Pickford M, Senut B. 2010. The geology, palaeontology and evolution of the Etosha Pan, Namibia: implications for terminal Kalahari deposition. *South African Journal of Geology* **113**: 307–334.

Muhs DR, Budahn JR, Prospero JM, Carey SN. 2007. Geochemical evidence for African dust inputs to soils of western Atlantic islands: Barbados, the Bahamas, and Florida. *Journal of Geophysical Researceh* **112**: F02009. https://orcid.org/10.1029/2005JF000445

Newman EI. 1995. Phosphorus inputs to terrestrial ecosystems. *Journal of Ecology* **83**: 713–726.

Okin GS, Reheis MC. 2002. An ENSO predictor of dust emission in the southwestern United States. *Geophysical Research Letters* **29**: 1332. https://orcid.org/10.1029/2001GL01449

Pabortsava K, Lampitt RS, Benson J, Crowe C, McLachlan R, Le Moigne FAC, Moore CM, Pebody C, Provost P, Rees AP, Tilstone GH, Woodward EMS. 2017. Carbon sequestration in the deep Atlantic enhanced by Saharan dust. *Nature Geoscience* **10**: 189–194.

Paris R, Desboeufs V, Journet E. 2011. Variability of dust iron solubility in atmospheric waters: investigation of the role of oxalate organic complexation. *Atmospheric Environment* **45**: 6510–6517.

Prospero JM, Ginoux P, Torres O, Nicholson SE, Gill TE. 2002. Environmental characterization of global sources of atmospheric soil dust identified with the NIMUS 7 total ozone mapping spectrometer (TOMS) absorbing aerosol product. *Reviews of Geophysics* **40**: 1002. https://orcid.org/10.1029/2000RG000095

Ramberg L, Hancock P, Lindholm M, Meyer T, Ringrose S, Sliva J, Van As J, Vander Post C. 2006. Species diversity of the Okavango Delta, Botswana. *Aquatic Sciences* **68**: 310–337.

Ramberg L, Lindholm M, Hesson DO, Murray-Hudson M, Bonyongo C, Heinl M, Masamba W, Vander Post C, Wolski P. 2010. Aquatic ecosystem responses to fire and flood size in the Okavango Delta: observations from the seasonal floodplains. *Wetlands Ecology and Management* **16**: 587–595.

Roberts G, Wooster MJ, Lagoudakis E. 2009. Annual and diurnal African biomass burning temporal dynamics. *Biogeosciences* **6**: 849–866.

Seymour CL, Milewski AV, Mills AJ, Joseph GS, Cumming GS, Cumming DHM, Mahlangu Z. 2014. Do the large termite mounds of *Macrotermes* concentrate micronutrients in addition to macronutrients in nutrient-poor African savannas? *Soil Biology and Biochemistry* **68**: 95–105.

Shi Z, Krom MD, Jickells TD, Bonneville S, Carslaw KS, Mihalopoulos N, Baker AR, Benning LG. 2012. Impacts on iron solubility in the mineral dust by processes in the source region and the atmosphere: a review. *Aeolian Research* **5**: 21–42.

Shi Y, Matsunaga T, Saito M, Yamaguchi Y, Chen X. 2015. Comparison of global inventories of CO_2 emissions from biomass burning during 2002–2011 derived from multiple satellite products. *Environmental Pollution* **206**: 479–487.

Sinha P, Hobbs PV, Yokelson RJ, Blake DR, Gao S, Kirchstetter TW. 2003. Distributions of trace gases and aerosols during the dry biomass burning season in southern Africa. *Journal of Geophysical Research* **108**(D17): 4536. https://orcid.org/10.1029/2003JD003691

Soderberg K, Compton JS. 2007. Dust as a nutrient source for fynbos ecosystems, South Africa. *Ecosystems* **10**: 550–561.

Sterner RW. 2008. On the Phosphorus Limitation Paradigm for Lakes. *International Review of Hydrobiology* **93**: 433–445.

Stockdale A, Krom MD, Mortimer RJG, Benning LG, Carslaw KS, Herbert RJ, Shi Z, Myriokefalitakis S, Kanakidou M, Nenes A. 2016. Understanding the nature of atmospheric acid processing of mineral dusts in supplying bioavailable phosphorus to the oceans. *Proceedings of the National Academy of Sciences of the USA* **113**: 14639–14644.

Sun D, Bloemendal J, Rea DK, Vandenberghe J, Jiang F, An Z, Su R. 2002. Grain-size distribution function of polymodal sediments in hydraulic and aeolian environments, and numerical partitioning of the sedimentary components. *Sedimentary Geology* **152**: 263–277.

Swap R, Garstang M, Greco S. 1992. Saharan dust in the Amazon basin. *Tellus* **B44**: 133–149.

Thomas DSG, Shaw PA. 1990. The deposition and development of the Kalahari Group sediments, Central Southern Africa. *Journal of African Earth Sciences* **10**: 187–197.

Thomas DSG, Shaw PA. 1991. *The Kalahari Environment*. Cambridge University Press: Cambridge.

Tyson PD, Garstang M, Swap R. 1996. Large-scale circulation of air over southern Africa. *Journal of Applied Meteorology* **35**: 2218–2236.

Vickery KJ, Eckardt FD, Bryant RG. 2013. A sub-basin scale dust plume source frequency inventory for southern Africa, 2005–2008. *Geophysical Research Letters* **40**: 5274–5279.

Vitousek PM, Porder S, Houlton BZ, Chadwick OA. 2010. Terrestrial phosphorus limitation: mechanisms, implications, and nitrogen-phosphorus interactions. *Ecological Applications* **20**: 5–15.

Wang L, D'Odorico P, Ringrose S, Coetzee S, Macko SA. 2007. Biogeochemistry of Kalahari sands. *Journal of Arid Environments* **71**: 259–279.

Wang L, D'Odorico P, Okin GS, Macko SA. 2009. Isotope composition and anion chemistry of soil profiles along the Kalahari Transect. *Journal of Arid Environments* **73**: 480–486.

Wang R, Balkanski Y, Boucher O, Ciais P, Peñuelas J, Tao S. 2014. Significant contribution of combustion-related emissions to the atmospheric phosphorus budgets. *Nature Geoscience* **8**: 48–54.

Washington R, Todd M, Middleton NJ, Goudie AS. 2003. Dust-storm source areas determined by the total ozone monitoring spectrometer and surface observations. *Annals of the American Association of Geographers* **93**: 297–313.

Wedepohl KH. 1995. The composition of the continental crust. *Geochimica et Cosmochimica Acta* **59**: 1217–1232.

Wilson BH, Dincer T. 1976. An introduction to the hydrology and hydrography of the Okavango Delta. In *Proceedings of the Symposium on the Okavango Delta and its Future Utilisation*. Botswana Society: Gaborone; 33–48.

Supporting Information

Additional supporting information may be found online in the Supporting Information section at the end of the article.

Table S1. Extractable iron and phosphorus concentrations